Spectroscopic Characterization and the Effect of Metal Ions on Langmuir–Blodgett Films of Octasubstituted Calix[4]resorcinarenes

W. C. Moreira,† P. J. Dutton,* and R. Aroca

Department of Chemistry and Biochemistry, University of Windsor, 401 Sunset, Windsor, Ontario N9B 3P4, Canada

Received January 25, 1995. In Final Form: May 10, 1995®

Calix[4]resorcinarenes octafunctionalized with methyl α-acetate (CALES) or methyl α-acetamide (CALAM) have been used to form Langmuir–Blodgett (LB) films on several different substrates. Spectroscopic characterization of these species as solids, solutions, and LB films were carried out using FT-IR, FT-Raman, UV–visible, and fluorescence spectroscopies. Considering the spectroscopic evidence, the conformation of both CALES and CALAM in the LB films was found to be the flattened cone. It has been shown that the presence of metal cations in the subphase results in incorporation of cations into the LB film. The film organization of the octafunctionalized calix[4]resorcinarene in the film is determined by the metal cation.

Interest in Langmuir–Blodgett (LB) films has led to several investigations of different types of materials that may be deposited to form monomolecular layers.[1] Classical examples include the families of long chain fatty acids and alcohols.[1] More recent developments in the field include species such as polymers, aromatic hydrocarbons, and dye substances.[2,3] Ordered systems have proven useful in applications such as molecular electronics, molecular optics, and chemical sensors.[2,4–6] For some applications, as in sensors, it is important to have a material with controlled thickness and organization. This goal can be achieved using the LB technique for the fabrication of films with defined molecular orientation.

The calixarenes and calixresorcinarenes have received much attention in a wide variety of areas.[7–10] These macrocycles and their derivatives form complexes with metal cations in manners similar to crown ethers and other compounds with defined cavities. Such species have polar cavities that are able to coordinate metal ions and often exhibit charge or size selectivity. These properties have been exploited in areas such as the fabrication of ion-selective electrodes[11,12] and foam fractionation of cesium ion from a mixture of alkali metal ions.[13] The calix[4]arene derivatives can act to transport cations across membranes[14,15] and there is also potential for their use as catalysts in a variety of systems.[16–19]

Calix[4]resorcinarene and several calixarenes have been shown to form stable monolayers.[20,21] In our previous work with *C*-undecylcalix[4]resorcinarene (CALOL), **1**, it was found that stable LB films with different spectroscopic behavior were obtained depending upon the spreading solvent.[22]

In related work, the complexation properties of octasubstituted calix[4]resorcinarenes in bulk solution toward metal cations have been studied. The synthesis, chemical characterization, and determination of the association constants of the octasubstituted calix[4]resorcinarenes have been carried out and will be reported elsewhere.

In this work we report the formation of Langmuir monolayers and the fabrication of Langmuir–Blodgett films of *C*-undecylcalix[4]resorcinarene octa-α-(diethyl acetamide) (CALAM) and octa-α-(methyl acetate) (CALES) and the effect of various metal ions in the subphase. The study with the ester and amide derivatives of these compounds may lead to a new class of sensors for alkali metals, alkaline earth and transition metals.

Experimental Section

The syntheses of octafunctionalized calix[4]resorcinarenes CALAM and CALES, shown in Scheme 1, were carried out in high yield using a modification of Ungaro's method for the functionalization of calix[4]arene.[23] The etherification reactions were carried out in 100% THF and yields were found to be between 68 and 87%. Nuclear magnetic resonance and elemental analysis

† Present address: Departamento de Quimica, Universidade Federal de São Carlos, C. P 676, 13565-905 São Carlos, SP, Brazil.

® Abstract published in *Advance ACS Abstracts,* July 1, 1995.

(1) *Langmuir-Blodgett Films*, 1st ed.; Roberts, G., Ed.; Plenum: New York, 1990; pp 425.
(2) Peterson, I. R. *J. Phys. D: Appl. Phys.* **1990**, *23*, 379–395.
(3) Sauer, T.; Arndt, T.; Batchelder, D. N.; Kalacher, A. A.; Wegner, G. *Thin Solid Films* **1990**, *187*, 357–374.
(4) Wang, H.-Y.; Lando, J. B. *Langmuir* **1994**, *10*, 790–796.
(5) Aroca, R.; Bolourchi, H.; Battisti, D. *Langmuir* **1993**, *9*, 3138–3141.
(6) Sauer, T.; Caseri, W.; Wegner, G.; Vogel, A.; Hoffmann, B. *J. Phys. D: Appl. Phys.* **1990**, *23*, 79–84.
(7) Perrin, R.; Lamartine, R.; Perrin, M. *Pure Appl. Chem.* **1993**, *7*, 1549–1559.
(8) McKervey, A. *Chem. Britain* **1992**, *7*, 724–727.
(9) *Calixarenes: A Versatile Class of Macrocyclic Compounds*; Vicens, J., Böhmer, V., Ed.; Kulwer: 1991; Vol. 3, pp 263.
(10) Gutsche, C. D. *Calixarenes*; Royal Society of Chemistry: Cambridge, 1989; Vol. 1, pp 223.
(11) Diamond, D.; Svehla, G.; Seward, E. M.; McKervey, M. A. *Anal. Chim. Acta* **1988**, *204*, 223–231.
(12) Sakaki, T.; Harada, T.; Deng, G.; Kawabata, H.; Kawahara, Y.; Shinkai, S. *J. Incl. Phenom. Mol. Recogn.* **1992**, *14*, 285–302.
(13) Koide, Y.; Oka, T.; Imamura, A.; Shosenji, K.; Yamada, K. *Bull. Chem. Soc. Jpn.* **1993**, *66*, 2137–2142.
(14) Chang, S.-K.; Hwang, H.-S.; Son, H.; Youk, J.; Kang, Y. S. *J. Chem. Soc., Chem. Commun.* **1991**, 217–218.
(15) Connor, M. D.; Janout, V.; Kudelka, I.; Dedek, P.; Zhu, J.; Regen, S. L. *Langmuir* **1993**, *9*, 2389–2397.
(16) Komiyama, M.; Isaka, K.; Shinkai, S. *Chem. Lett.* **1991**, 937–940.
(17) Shinkai, S.; Mori, S.; Koreishi, H.; Tsubaki, T.; Manabe, O. *J. Am. Chem. Soc.* **1986**, *198*, 2409–2416.
(18) Nomura, E.; Taniguchi, H.; Otsuji, Y. *Bull. Chem. Soc. Jpn.* **1994**, *67*, 309–311.
(19) Nomura, E.; Taniguchi, H.; Otsuji, Y. *Bull. Chem. Soc. Jpn.* **1994**, *67*, 792–799.
(20) Nakamoto, Y.; Kallinowski, G.; Böhmer, V.; Vogt, W. *Langmuir* **1988**, *4*, 276.
(21) Ishikawa, Y.; Kunitake, T.; Matsuda, T.; Otsuka, T.; Shinkai, S. *J. Chem. Soc., Chem. Commun.* **1989**, 736–738.
(22) Moreira, W. C.; Dutton, P. J.; Aroca, R. *Langmuir* **1994**, *10*, 4148–4152.
(23) Arduini, A.; Pochini, A.; Reverberi, S.; Ungaro, R. *J. Chem. Soc., Chem. Commun.* **1984**, 981–982.

0743-7463/95/2411-3137$09.00/0

Scheme 1. Synthesis of Octafunctionalized Calix[4]resorcinarenes

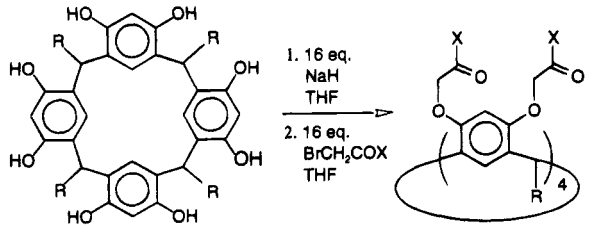

CALOL
R = $C_{11}H_{23}$

CALES X = OMe
CALAM X = NEt_2

data were consistent with the complete functionalization of the phenolic groups.

The π–A isotherms of CALES and CALAM were recorded at 15 and 25 °C. Solvents used to prepare spreading solutions were glass-distilled HPLC grade chloroform from EM Science and spectrophotometric grade toluene from Aldrich. Chloroform was dried over activated 4A molecular sieves prior to use. Monolayers were spread onto a Lauda Langmuir Film Balance equipped with a Lauda Fl-1 electronically controlled dipping device using 2×10^{-4} M solutions in chloroform or toluene. The subphases were double distilled water, passed through a Milli-Q Plus filtration system, with final resistivity of 18.2 MΩ cm, and solutions of the following salts (2×10^{-4} M): KCl, NaCl, $CaCl_2$, $BaCl_2$, $AgNO_3$, $CuCl_2$, $CdCl_2$, and $HgCl_2$. All salts were AnalaR grade obtained from BDH and were used without further purification. Arachidic acid (puriss) was obtained from Fluka. Isotherms of mixed monolayers were recorded for CALAM using chloroform solutions of arachidic acid (AA) and CALAM in proportions of 5:1 and 1:3 CALAM:AA. All π-A isotherms were recorded 30 min after spreading to allow solvent evaporation and/or interaction with the subphase. The barrier velocity was 2 mm min^{-1}, which corresponded to a compression rate of 0.012 and 0.025 nm^2 $molecule^{-1}$ min^{-1} for CALES and CALAM, respectively. The LB monolayers were transferred to substrates at 25°C in the vertical mode at a deposition rate of 2 mm min^{-1} and a surface pressure of 25 mN m^{-1}. Substrates included quartz, zinc sulfide, germanium, and smooth silver film (100 nm thickness) substrates.

Electronic absorption spectra were obtained on a Response UV–vis spectrophotometer interfaced to an IBM PC. The spectra were recorded from KBr pellets, two LB monolayers (02 LB) on quartz (one on each side of the substrate), and chloroform or toluene solutions.

Infrared spectra were recorded using a BOMEM DA3 FT-IR spectrometer. Spectra were obtained from KBr pellet (resolution 1 cm^{-1}), LB films (resolution of 4 cm^{-1}) on ZnS or Ge and 07 LB on smooth silver film. Both transmission and reflection–absorption spectra were obtained. The reflection–absorption spectrum of CALES taken from an aqueous copper(II) subphase onto a smooth silver film was collected using a Spectra-Tech Inc. Model 500 accessory with an angle of incidence of 80°.

A BOMEM RAMSPEC 150 spectrophotometer with an Nd/YAG laser emitting at 1064.1 nm was used to obtain the FT-Raman spectra from powders in glass capillaries.

The emission spectra of samples in KBr pellets or chloroform solutions were recorded using a SPEX 1403 spectrometer equipped with a Spectra Physics Model 164 Ar^+ laser operating at 488 nm.

Results and Discussion

Isotherms. Figures 1 and 2 show the π–A isotherms for CALES and CALAM with a pure water subphase at 15 and 25 °C. It was not possible to obtain reproducible isotherms at 25 °C from CALES using chloroform as the spreading solvent. The small values for the collapse pressure of CALES (ca. 30 mN m^{-1}) when compared with CALOL (ca. 45 mN m^{-1})[22] indicate a weaker interaction between the film-forming molecules due to the lack of direct intermolecular hydrogen bonding and thus an increasing ability to "fold over". The distinctly different

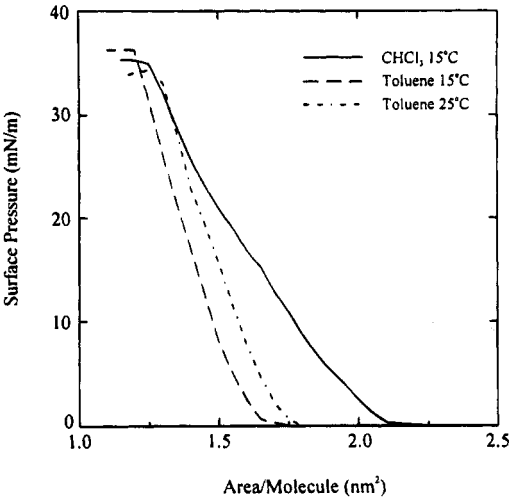

Figure 1. π–A isotherms of CALES using chloroform and toluene as the spreading solvents at 15 and 25 °C.

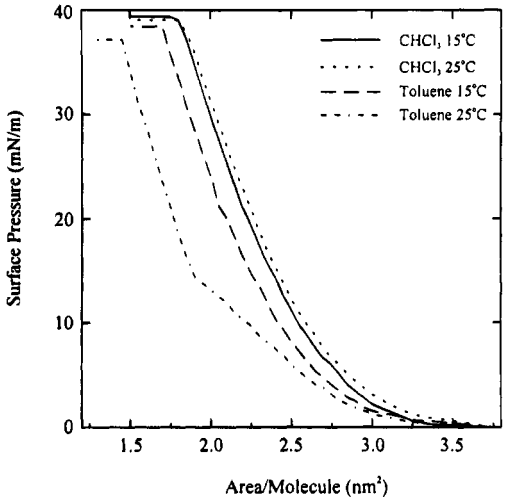

Figure 2. π–A isotherms of CALAM using chloroform and toluene as the spreading solvents at 15 and 25 °C.

shape of the isotherms at 15 °C, as a result of the change in spreading solvent, and the inability to obtain a stable Langmuir film at 25 °C from $CHCl_3$ solution indicate that the solvent has an effect on the packing arrangement of the Langmuir films.[24–26]

The limiting area values were obtained by extrapolation from the region of high pressure to zero surface pressure and are shown in Table 1. CALAM showed larger values of limiting areas than CALES, as would be expected due to the relative size of the amide functional group compared to the methyl ester. Figure 2 shows that there was a significant effect on the π–A isotherms as a result of the change in the spreading solvent. Approximately superimposable isotherms for CALAM were obtained, independent of temperature, when chloroform solution was used to spread the monolayer. When toluene solution was used, a liquid expanded to liquid condensed phase transition was observed at 25 °C that was clearly not manifested at 15 °C. This behavior is the same as that observed for CALOL[22] and is consistent with the experimental observation that the spreading solvent may

(24) Gobernado-Mitre, M. I.; Aroca, R.; De Saja, J. A. *Langmuir* **1995**, in press.
(25) Gabrielli, G.; Baglioni, P.; Ferroni, E. *Colloid Polym. Sci.* **1979**, *257*, 121–127.
(26) Gericke, A.; Simon-Kutscher, J.; Hühnerfuss, H. *Langmuir* **1993**, *9*, 2119–2127.

Table 1. Limiting Area Values of CALES and CALAM on Several Subphases[a]

	Limiting area/molecule (nm^2)										
	H_2O (tol)[b]		H_2O (chl)[b]								
subphase	15 °C	25 °C	15 °C	25 °C	Na^+	K^+	Ba^{2+}	Ag^+	Cd^{2+}	Hg^{2+}	Cu^{2+}
CALES	1.56	1.65	1.78		1.65	1.61	1.63	1.63	1.65	1.63	1.65
CALAM	2.50	2.15	2.65	2.70	2.68	2.90	2.60	3.10	3.08	3.10	3.00

[a] Concentration of metal ion in the subphase ca. 2×10^{-4} M. [b] tol = toluene spreading solvent; chl = chloroform spreading solvent.

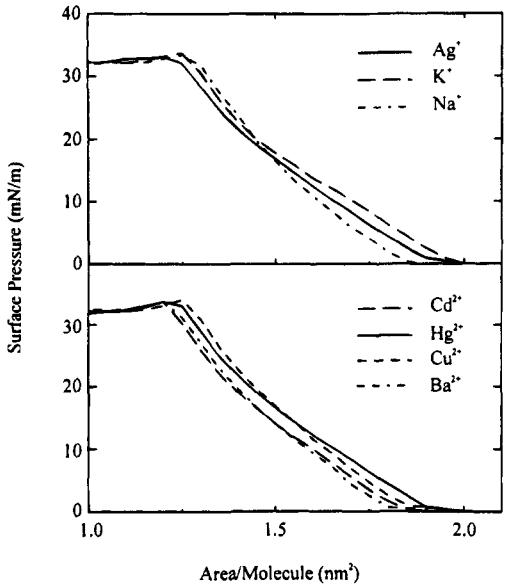

Figure 3. π–A isotherms of CALES (spreading solvent toluene) on subphases of metal cations (2 x 10^{-4} M) at 25 °C.

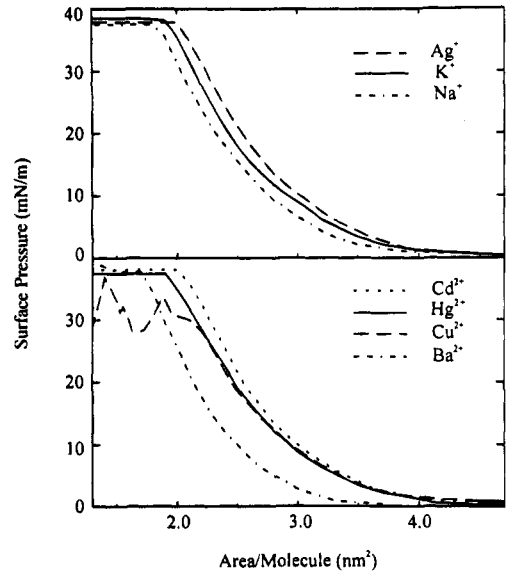

Figure 4. π–A isotherms of CALAM (spreading solvent chloroform) on subphases of metal cations (2×10^{-4} M) at 25 °C.

significantly effect the π–A isotherm.[24-26] Within the sensitivity of the absorption IR experiments of the LB films, IR active fundamentals due to the "solvent" molecules were not observed.

The CALES isotherms also show solvent dependent behavior; however, there is little effect on the final limiting area of the films prepared from different solvents. The increase in limiting area with a change in temperature from 15 to 25 °C (based upon $\pi A = ikT$) is typically small and this value is dependent upon the species involved. A 6% change is observed, which indicates that the films prepared from chloroform at the two temperatures are the same.

Considering thermodynamic arguments, it could be expected that the association equilibria for the interaction between the metal cations and the monolayer would be favored at higher temperature. For this reason the effects of the metal ions on the π–A isotherms were studied at a temperature of 25 °C. The choice of solvent used to spread the monolayer was based upon the largest observed value of the limiting area: toluene was chosen to spread CALES films and chloroform was used to spread CALAM films.

Figures 3 and 4 show the π–A isotherms for CALES and CALAM with various metal ions in the subphase. The minor changes in the limiting area for CALES, as shown in Table 1, do not allow us to differentiate CALES–metal ion interactions. Although the limiting area was not observed to change compared a pure aqueous subphase (Figure 1), the liquid expanded to liquid condensed phase transitions varied with the metal ion in the subphase (Figure 3). This may be the result of an interaction between CALES and the metal ion(s) in the subphase.

Figure 4 shows that in the case of CALAM, different behavior from CALES is observed. The liquid expanded to liquid condensed phase transition is not clearly observed in the CALAM isotherms. Table 1 shows that CALAM exhibits changes in the limiting area that were dependent upon the metal ion in the subphase.

Studies of the conformation of CALAM based upon CPK models indicate that the area per molecule of CALAM could change due to the orientation of the functional groups from 1.9 to 3.1 nm^2, assuming a flattened cone conformation, which was found to be one of two important conformations in CALOL.[22] The change in limiting area of CALES is very small for the same conformation (from 2.1 to 2.3 nm^2). The pendant functional groups could be entirely responsible for the different behavior observed between CALES and CALAM.

Mixed Monolayers. In contrast to CALES, it was not possible to obtain multilayers of CALAM from a pure aqueous subphase, or from subphases containing metal cations. A single monolayer of CALAM was taken on the first upstroke (transfer ratio (τ) = 1) and subsequent downstroke/upstroke cycles showed transfer ratios of zero. This indicated that the first monolayer is stable on the substrate, but that subsequent monolayers could not be lifted. No difference was observed when different substrates were used (glass, quartz, silver island, gold island, or ZnS). The use of mixed monolayers has been shown to improve the transfer of LB films. In order to transfer multilayers containing CALAM to a substrate, the use of mixed monolayers was explored.

The π–A isotherms of mixtures of CALAM with arachidic acid (AA) in two different mole ratios are shown in Figure 5. The limiting areas observed for the mixed isotherms of CALAM/AA were 4.2 nm^2 (5:1 CALAM:AA) and 0.8 nm^2 (1:3 CALAM:AA). A calculation of the theoretical limiting area for the two cases based upon the known limiting areas of CALAM (Table 1) and AA (0.24 nm^2)[1] gives values of 2.29 and 0.86 nm^2/molecule for 5:1 and 1:3 CALAM:AA, respectively. The high value of 4.2

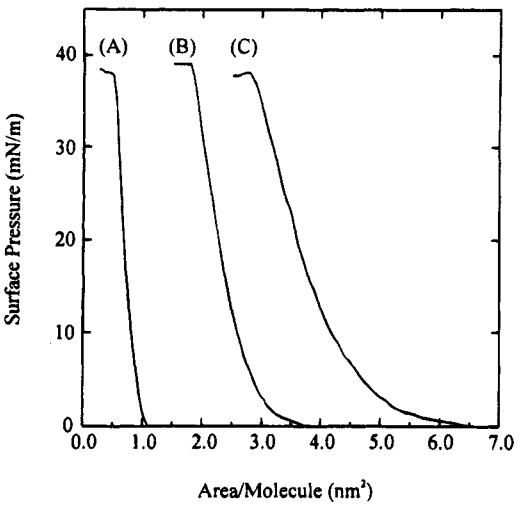

Figure 5. π–A isotherms of mixed monolayers of CALAM and arachidic acid: CALAM:arachidic acid ratio (A) 1:3, (B) 1:0, (C) 5:1 (spreading solvent chloroform).

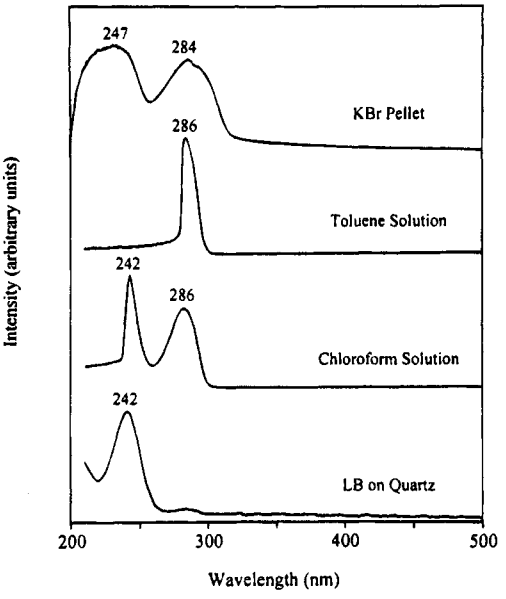

Figure 6. Electronic spectra of CALES.

nm² observed for 5:1 CALAM:AA is an indication that there is some interaction between AA and CALAM and suggests that the two species are not separated into different domains. The extent of mixing of the two species cannot be determined with certainty since domain visualization techniques were not applied to the Langmuir films. In the 1:3 CALAM:AA film, the theoretical limiting area and the observed limiting area are in agreement with one another.

It was only possible to obtain a single LB with a transfer ratio of unity on the first upstroke in both cases. In subsequent downstroke/upstroke cycles the transfer ratio was not zero but was very low ($\tau < 0.2$). Clearly the use of arachidic acid does not improve the transfer. The interaction of the AA and CALAM may disrupt the AA packing and prevent the good transfer that is often observed with mixed films of AA.

Electronic Spectra. The top traces in Figures 6 and 7 show the electronic spectra for CALES and CALAM as dispersions in KBr. CALES has two absorptions in the UV region centered at 284 and 247 nm. In previous work[22] the absorptions at 284 and 247 nm were assigned to two different conformations in the solid state, cone (C_{4v}) and flattened cone (C_{2v}), respectively. CALAM in the solid

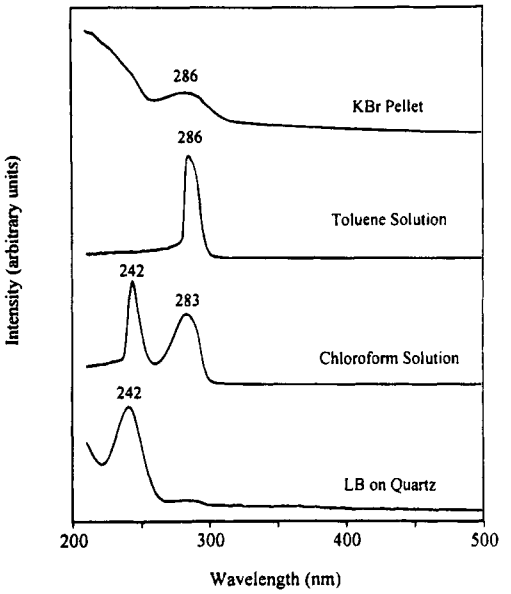

Figure 7. Electronic spectra of CALAM.

state shows a band at 286 nm and another absorption that rises into the instrument cutoff.

The electronic spectra in solution for both compounds, shown in the second and third traces, are similar. In toluene both CALES and CALAM show only a single absorption at 286 nm. In chloroform two absorptions for each compound were observed at 242 and 286 nm for CALES and 244 and 283 nm for CALAM.

The electronic spectra for LB films of both CALES and CALAM are shown in the bottom traces of Figures 6 and 7. The electronic spectra for the LBs of each compound were identical, independent of the temperature or the solvent used to spread the monolayer. When films were produced from CALOL, different conformations were obtained, depending on the spreading solvent.[22] In CALES and CALAM a single spectral form, corresponding to the flattened cone conformation, was obtained, probably due to the large mobility and weak inter- and intramolecular interactions of the functional groups. In the flattened cone conformation, two of the benzene rings disposed across the macrocycle from one another are approximately parallel to the surface of the substrate and the other two are approximately perpendicular.

The effects of metal ions in the subphase on the electronic spectra of monolayers of CALES and CALAM are shown in Figures 8 and 9. The UV–visible spectra of films of CALES from aqueous subphases containing Ba^{2+} and Ag^{+} are similar to the spectrum of the film obtained from a pure aqueous subphase. In these three cases, strong 240 nm bands and weak 284 nm bands were observed. This indicates that the conformation of the calixresorcinarene framework in the LB film was not effected by silver or barium ions. The spectra obtained from films taken from Na^{+}, K^{+}, and Cd^{2+} subphases are very similar to one another in that they all have a 284 nm band and a weak band at approximately 233 nm (observed as a shoulder on the instrument cutoff). The presence of Cu(II) in the subphase gives rise to a film with a UV spectrum that is somewhat similar to those obtained from Na^{+}, K^{+}, and Cd^{2+}. A band at 286 nm is observed, as is another band at 225 nm. The shift from the normally observed 240 nm band to the higher energy band in these cases could be due to a distortion of the flattened cone conformation. Mercury(II), however, caused a completely different spectrum for the LB film. The absorption in the 242 nm region was not clearly observed and the 282 nm band was extremely weak.

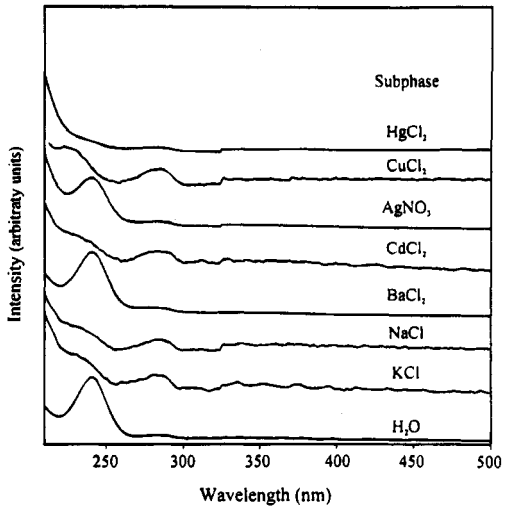

Figure 8. Electronic spectra of LB films of CALES on quartz.

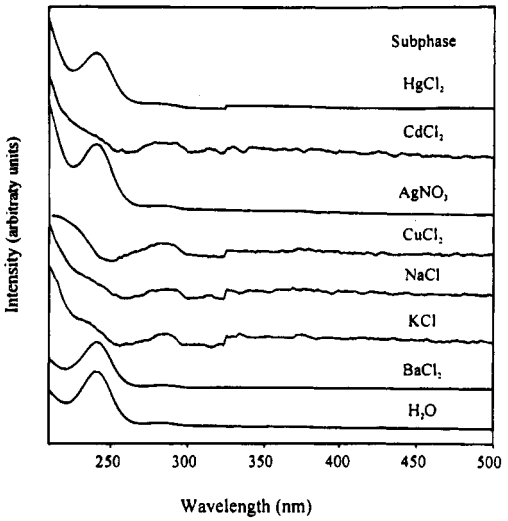

Figure 9. Electronic spectra of LB films of CALAM on quartz.

In these cases, even though the limiting areas are all the same, the UV spectra indicate that various metal ion–Langmuir film interactions have resulted in effects on the conformations observed for CALES in the Langmuir–Blodgett film.

The effects of the metal ions in the subphase on the UV spectra of LB films of CALAM were similar, except for Hg^{2+}, to the effects observed for CALES. The UV–visible spectra of films of CALAM from aqueous subphases containing Hg^{2+}, Ba^{2+}, and Ag^{+} were all very similar to the CALAM taken from pure water. A strong band at 240 nm and a weak band at 284 nm were observed in these cases, likely due to a preponderance of the flattened cone conformation in the LB films. The presence of Cd^{2+}, Na^{+}, or K^{+} in the subphase caused changes in the UV spectra of the CALAM LB film: the 240 nm band was not resolved due to the weakness of the signal, and the relative intensity at 284 nm increased. Copper(II) in the subphase again causes an anomalous change in the UV spectrum of the LB film. CALAM was found to have one band at 284 nm and another at approximately 235 nm.

The UV spectra of CALAM do not follow exactly the same trends as those observed for CALES. The data indicate that the conformation of CALAM in LB films also changes as a result of the presence of various metal ions in the subphase.

The emission spectra of either CALES or CALAM in KBr pellets using the 488 nm line produced a broad band

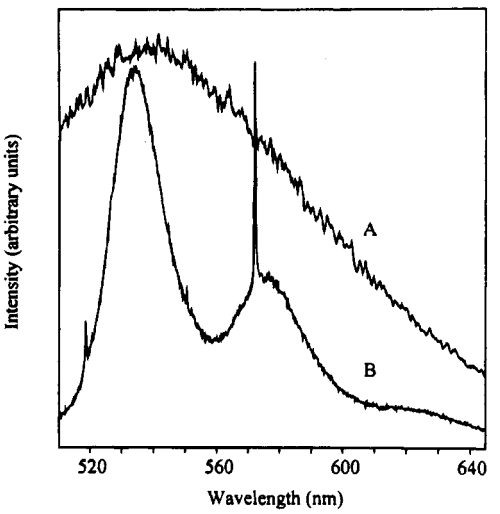

Figure 10. Emission spectra of CALAM in a (A) KBr pellet and (B) chloroform solution (excitation 488 nm).

probably associated with a phosphorescence process caused by the presence of a triplet state. A triplet state in the closely related calix[4]arenes has been assigned by Sabbatini,[27] though the phosphorescent band was not shifted as far from the electronic absorption as in the case of the calix[4]resorcinarenes. Upon dilution in chloroform solution, the broad features of the solid spectra resolved into two bands at 534 and 574 nm. These bands are in exactly the same positions in both CALES and CALAM and is therefore a transition involving the calixarene framework and not the pendant functional groups. The spectra for CALAM are shown in Figure 10.

Infrared Spectra. Figure 11 shows the infrared spectra of CALES in KBr pellet and LB films taken from several subphases. The spectrum from the KBr pellet (A) is the reference spectrum and shows the characteristic frequencies associated with alkyl chains, aromatic rings, and carbonyl functional groups. The FT-Raman spectrum of a powder sample of CALES is shown in Figure 12. Table 2 includes a tentative assignment of the observed fundamentals in the Raman and infrared spectra of CALES (subsequent reference to the individual spectra is understood to include a reference to Table 2).

The symmetric (2851 cm^{-1}) and antisymmetric (2924 cm^{-1}) C–H stretching frequencies associated with the methylene groups observed in the infrared were also observed in the Raman spectrum, although in the Raman spectrum the symmetric mode is more intense than the antisymmetric mode. It was also observed that the intense Raman band of the symmetric CH_3 stretching vibration (2882 cm^{-1}) was not observed in the infrared.

Two strong characteristic bands of CO stretching modes (1763 and 1732 cm^{-1}) were seen from the eight carbonyls in the molecule. These two bands are also present in the Raman spectrum (1765 and 1735 cm^{-1}) with very weak relative intensity.

Spectrum B in Figure 11 shows the infrared spectrum of 24 LB of CALES on ZnS transferred from pure water as subphase. The changes in relative intensities observed in spectrum B compared to the reference KBr pellet (spectrum A) are due to the molecular organization in the LB film. In the transmission geometry, vibrational transitions with a dipole moment component parallel to the surface of the film should be observed with considerable relative intensity. Therefore, the spectrum B indicates,

(27) Sabbatini, N.; Guardigli, M.; Mecati, A.; Balzani, V.; Ungaro, R.; Ghidini, E.; Casnati, A.; Pochini, A. *J. Chem. Soc., Chem. Commun.* **1990**, 878–879.

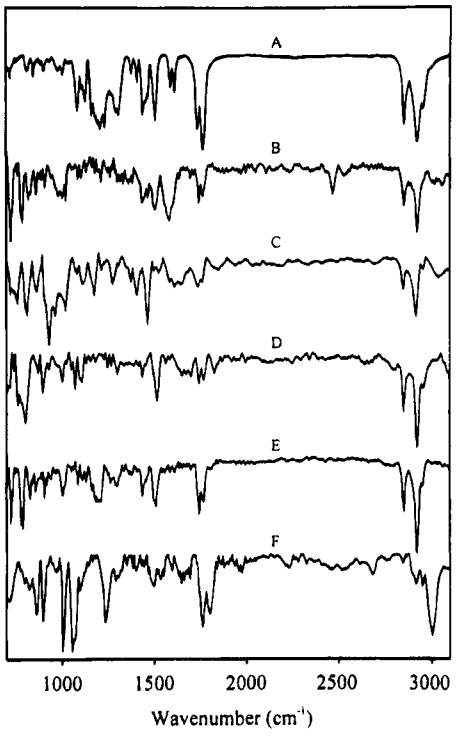

Figure 11. Infrared spectrum of CALES: (A) KBr pellet; (B) 24 LB on ZnS; (C) 18 LB on Ge ($AgNO_3$ subphase); (D) 24 LB on ZnS ($HgCl_2$ subphase); (E) 24 LB on ZnS ($CuCl_2$ subphase, transmission geometry); (F) 7 LB on smooth silver film ($CuCl_2$ subphase, RAIR).

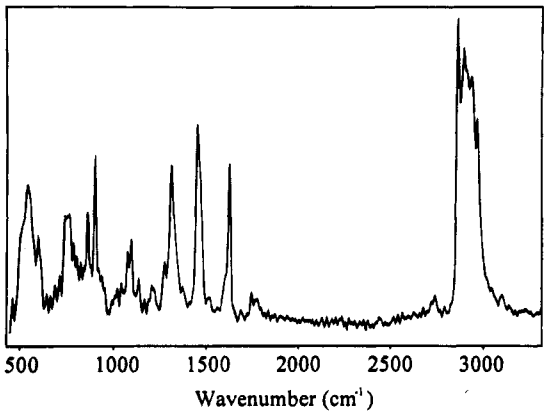

Figure 12. FT-Raman of CALES.

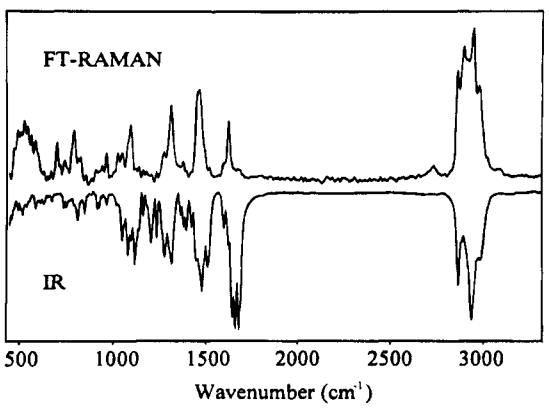

Figure 13. FT-Infrared and FT-Raman of CALAM.

qualitatively, that the CH_2 groups have a large transition moment component parallel to the surface, while the C=O groups are tilted and closer to the surface normal.

In the spectrum of the CALES LB film lifted from an aqueous subphase, the relative intensity of the tangential benzene vibration (ν_8, 1581 cm^{-1}) was enhanced in the transmission geometry relative to the radial vibration (ν_{19}, 1504 cm^{-1}) and the carbonyl bands. In the cone conformation it was expected that ν_{19} would be much stronger than ν_8, as was observed in the unsubstituted calix[4]-resorcinarene.[22]

The transmission infrared spectra of LB films taken from aqueous subphases of $AgNO_3$ (18 LB on Ge), $HgCl_2$ (24 LB on ZnS), and $CuCl_2$ (24 LB on ZnS) are also shown in parts C, D, and E, respectively, of Figure 10.

The symmetric and antisymmetric stretching vibrations for the alkyl chain observed in the spectrum of LB film taken from the Ag^+ subphase show an ordered *trans*–zig-zag conformation[28] (ν_s = 2851 cm^{-1}, ν_{as} = 2918 cm^{-1}). In contrast, the alkyl chains in the LB films obtained from Hg^{2+} or Cu^{2+} show a higher degree of disorder (ν_s = 2852 cm^{-1}, ν_{as} = 2924 cm^{-1}).

Spectra C (Ag^+) and D (Hg^{2+}) of Figure 11 show significant changes in the carbonyl region when compared with spectrum B (neat film). The bands at 1682 and 1641 cm^{-1} in C and 1699, 1670, and 1651 cm^{-1} in D may be assigned to the carbonyl stretching modes in the metal complexes. The carbonyl stretching bands at 1765 and 1735 cm^{-1} (in all spectra) indicate the presence of carbonyls that are not associated with a metal ion. The pattern observed for the carbonyl bands in spectra C and D indicate that Hg^{2+} has a different coordination than Ag^+.

The transmission spectrum of the LB film taken from a Cu^{2+} subphase does not reveal any new carbonyl bands; however, it was apparent that there were changes in other regions of the mid-IR. Five new bands of medium intensity at 1456, 1296, 1288, 1103, and 916 cm^{-1} were present in the transmission spectrum of the film taken from the copper subphase (spectrum E) which were not present in the film obtained from a pure water subphase (spectrum B). Also a shift of the 1022 cm^{-1} band in spectrum B to 1016 cm^{-1} in spectrum E was noted. Finally, it was observed that differences in the relative intensities for the two carbonyl bands in the copper spectrum compared to spectrum B follow the trend observed for all metal complexes.

Spectrum F, which was recorded in the reflection absorption geometry, did reveal the presence of new carbonyl bands at lower frequencies, as was observed for the other metal complexes in the transmission geometry. These results indicated that the Cu^{2+} ion was also associated with CALES.

The benzene stretching vibrations ν_8 and ν_{19} are also affected by the metal complexes in the LB films. In spectrum D for the Hg^{2+} complex, the ν_8 band (1600 cm^{-1}) is absent. The second ν_8 band (1583 cm^{-1}) is of very low intensity. A new band was observed at 1562 cm^{-1} that may be due to a shift of the ν_8 benzene stretch as a result of the direct interaction between the metal ion and the aromatic rings. The other metal ions also exhibit effects on the aromatic ring vibrations but not in exactly the same manner as in the Hg^{2+} case. In the Ag^+ film the original ν_8 bands are present, and a new band at lower wavenumber (1524 cm^{-1}) was observed. In the Cu^{2+} film, no new bands are observed, but a decrease in the intensity of the ν_8 bands was apparent, suggesting a change in the orientation of the aromatic rings.

The infrared and FT-Raman spectra of CALAM are shown in Figure 12. The CH stretching region of the spectrum is very similar to that obtained from CALES. One slight change in the infrared C–H stretching region

(28) Sapper, H.; Cameron, D. G.; Mantsch, H. H. *Can. J. Chem.* **1981**, *59*, 2543–2549.

Table 2. Characteristic Frequencies of CALES in the Infrared and Raman

FT-IR							
KBr pellet[a]	H_2O[b] subphase 24 LB	$AgNO_3$[b] subphase 18 LB	$HgCl_2$[b] subphase 24 LB	$CuCl_2$[b] subphase 24 LB	$CuCl_2$[c] subphase 07 LB	FT-Raman powder	assignments
	3018 (26)	3036 (23)				3088 (6)	C–H stretch (aromatic)
	3003 (23)				3003 (85)		C–H stretch (aromatic)
2954 (48)	2949 (26)	2957 (13)	2957 (39)	2951 (26)	2951 (33)	2955 (66)	C–H $\nu_{as}(CH_3)$
2924 (86)	2924 (79)	2918 (67)	2924 (100)	2922 (100)	2918 (30)	2924 (81)	C–H $\nu_{as}(CH_2)$
	2879 (26)						C–H $\nu_s(CH_3)$
2851 (64)	2852 (49)	2851 (36)	2852 (61)	2852 (54)	2847 (9)	2849 (100)	C–H $\nu_s(CH_2)$
		1846 (12)	1824 (21)		1799 (61)		ν(C=O)
1763 (100)	1765 (36)	1759 (27)	1767 (29)	1766 (44)	1763 (75)	1765 (6)	ν(C=O)
1732 (70)	1741 (45)	1736 (33)	1742 (32)	1741 (58)	1741 (37)	1735 (8)	ν(C=O)
		1682 (16)	1699 (25)	1695 (7)	1693 (24)		ν(C=O)
			1670 (21)				ν(C=O)
		1641 (30)	1651 (25)		1645 (28)		ν(C=O)
1611 (30)	1601 (47)	1608 (33)		1610 (12)		1613 (53)	benzene (ν_8)
					1594 (15)		benzene ($\nu_{8a,8b}$)
1588 (26)	1581 (64)	1583 (28)	1583 (7)	1583 (11)			benzene (ν_8)
			1562 (11)				
		1524 (17)	1516 (50)				
1506 (59)	1504 (53)			1506 (49)			benzene (ν_{19})
		1499 (14)	1494 (21)	1498 (40)	1495 (31)		benzene (ν_{19})
1467 (36)	1465 (40)	1467 (76)		1463 (16)			CH_2 deformation
1455 (41)				1456 (23)			CH_2 deformation
1438 (53)	1435 (45)		1437 (25)	1437 (37)			CH_2 deformation
1409 (21)		1406 (42)					CH_3 deformation
1378 (14)	1383 (23)	1375 (27)		1375 (14)			CH_3 deformation
1307 (53)	1302 (21)	1304 (9)	1302 (21)		1303 (22)		CH_2 wag
1292 (50)				1296 (25)		1299 (50)	benzene (ν_{14})
		1275 (29)		1288 (26)	1288 (27)		benzene (ν_{14})
1265 (33)	1261 (17)		1267 (14)	1259 (23)		1264 (17)	CH_2 twist
1231 (68)	1246 (11)		1248 (14)	1247 (14)	1234 (70)		ν(C–O)
1207 (70)	1211 (23)	1213 (14)		1211 (44)			ν((O=C)–O–CH_3)
1194 (63)	1198 (11)			1197 (44)		1195 (9)	C–H benzene bend
1181 (57)	1178 (13)	1176 (42)		1180 (44)			CH benzene bend
1161 (54)				1163 (30)			CH benzene bend
1127 (40)	1130 (11)			1130 (21)			CH benzene bend
1107 (28)		1117 (29)	1107 (29)	1111 (21)			$\nu(CH_2–O)$
			1097 (29)	1103 (23)	1095 (36)		CH benzene bend
1084 (49)	1085 (19)	1082 (17)		1086 (28)		1083 (24)	ν_{as}(O–CH_3)
	1076 (11)	1072 (14)	1072 (39)	1078 (16)			CH benzene bend
	1061 (11)			1061 (9)	1068 (90)	1064 (20)	CH benzene bend
	1051 (9)		1051 (18)	1051 (9)	1057 (100)		CH benzene bend
	1022 (45)	1020 (59)	1024 (11)	1016 (26)			CH benzene bend
1006 (15)	1005 (45)		1001 (29)	1003 (35)	1005 (100)		δ_{12}(C–C–C trigonal bend)
	968 (30)	964 (66)					
	941 (17)	932 (100)	930 (18)	939 (18)			
				916 (26)			
902 (12)	906 (28)		897 (43)	905 (42)	897 (69)		δ(CH out of plane)
886 (7)	862 (36)	866 (37)	872 (39)	856 (33)	862 (61)	888 (52)	
811 (13)	816 (45)	816 (66)		818 (28)			
	791 (62)		802 (75)	789 (75)	797 (28)		δ(CH out of plane)
	779 (74)		781 (54)	779 (75)			ring pucker
		760 (51)	762 (54)				
	733 (64)		741 (18)	735 (46)		747 (29)	ring breathing
721 (19)	725 (100)	722 (42)	719 (36)	725 (35)	716 (48)		CH_2 rock
		681 (50)					
		652 (50)					
					542 (100)		

[a] Relative intensities are given in parentheses. [b] Transmission geometry. [c] RAIRS on silver.

was that the antisymmetric stretch of CH_3 was observed at higher wavenumber than in CALES (2971 cm^{-1}) due to the presence of different CH_3 groups (NCH_2CH_3). In the Raman spectrum both of the C–H antisymmetric stretching modes (CH_2 and CH_3) were observed at higher wavenumber than those observed for CALES.

CALAM shows four bands in the carbonyl stretching region at 1675, 1667, 1647, and 1633 cm^{-1}, which was an indication of the lower symmetry of CALAM relative to CALES.

The other regions of the CALAM spectrum are nearly identical with CALES and were assigned on that basis. Some new bands are observed in the KBr pellet of CALAM that were characteristic of the amide functional group. The CH_3 deformation of the ethyl group (1365 cm^{-1}), CH_2–N stretch (1220 cm^{-1}), N–CH_2 twist (1147 cm^{-1}), C–C–N and C–N–C bending modes (1066–911 cm^{-1}) are all present. The tentative assignment of the fundamental vibrational frequencies observed in the infrared and FT-Raman spectra are given in Table 3.

Conclusion

It has been shown that the octafunctionalized calix[4]-resorcinarenes, CALES and CALAM, form stable Langmuir films. The limiting area values are in good agree-

Table 3. Characteristic Frequencies of CALAM in the Infrared and Raman

IR KBr pellet[a]	FT-Raman powder[a]	assignments
	3065 (6)	C–H stretch (aromatic)
2971 (41)	2967 (62)	C–H $\nu_{as}(CH_3)$
2923 (88)	2934 (100)	C–H $\nu_{as}(CH_2)$
2870 (30)	2882 (88)	C–H $\nu_s(CH_3)$
2851 (60)	2849 (72)	C–H $\nu_s(CH_2)$
1675 (83)		ν(C=O, amide I)
1667 (100)	1669 (8)	ν(C=O, amide I)
1647 (97)	1657 (9)	ν(C=O, amide I)
1633 (86)		ν(C=O, amide I)
1610 (31)	1611 (40)	benzene (ν_8)
1585 (21)	1588 (13)	benzene (ν_8)
1498 (48)	1508 (10)	benzene (ν_{19})
1467 (64)		CH_2 deformation
1436 (42)	1449 (60)	CH_2 deformation
1410 (20)	1408 (7)	CH_3 deformation
1381 (21)	1381 (8)	CH_3 deformation
1365 (20)	1366 (14)	$\delta_s(CH_3)$ of CH_3CH_2
1349 (13)		CH_2 bending
1302 (44)		CH_2 wag
1292 (sh)	1298 (50)	benzene (ν_{14})
1262 (40)	1262 (20)	ν(C–O)
1220 (27)	1220 (7)	$\nu(CH_2–N)$
1192 (30)		C–H benzene bend
1147 (15)		NCH_2 twist
1126 (23)		C–H benzene bend
1104 (44)		$\nu(CH_2–O)$
1081 (28)	1080 (37)	C–H benzene bend
1066 (38)		δ(C–C–N–C–C)
1036 (29)	1034 (19)	δ(C–C–N–C–C)
1002 (7)	1011 (19)	δ_{12}(C–C–C trigonal bend)
952 (7)	952 (19)	δ(C–C–N–C–C)
948 (7)		δ(C–C–N–C–C)
911 (11)		δ(C–C–N–C–C)
899 (9)		δ(CH out of plane)
834 (12)		C–H wag
793 (16)	799 (16)	$\varrho(CH_2–N)$
772 (8)	776 (33)	CH_2 rock
721 (10)	727 (14)	ring breathing
656 (5)	655 (7)	β(O=C–N)
618 (7)	618 (7)	
613 (7)		
569 (6)		β(O=C–N)

[a] Relative intensities are given in parentheses.

ment with the expected values for both compounds based upon CPK model studies.

Multilayer films of CALES on several different substrates were obtained, but it was only possible to obtain a single monolayer film of CALAM. The isotherms of mixed monolayers of CALAM and arachidic acid indicate a strong interaction between the two compounds.

The electronic spectra of both CALES and CALAM showed that the predominant form in the LB film was attained independent of both temperature and solvent conditions used in the LB fabrication. The major conformation in the LB films of both species was assigned as the flattened cone.

The infrared spectra in transmission geometry were obtained for CALES, and it was shown that the metal cations seem to be bound mainly to the carbonyl functional groups. The flattened cone conformation allows four of the carbonyl oxygens on the "perpendicular" aromatic rings to participate in an ion–dipole binding interaction with the cation. These interactions are currently being explored in homogeneous solution by nuclear magnetic resonance techniques and will be reported elsewhere. In addition, there was evidence for significant interactions by Hg^{2+}, Cu^{2+}, and Ag^{+} with the aromatic rings. Mercury had a strong effect on the characteristic aromatic ring vibrations, in agreement with the lack of a significant electronic transition in the spectrum of the LB film, suggesting that Hg^{2+} is bound not only to the carbonyl oxygens but also to the aromatic ring(s). Using the electronic spectra as an indication of changes in conformation, it is found that the metal cations Hg^{2+}, Cu^{2+}, Cd^{2+}, Na^{+}, or K^{+} affected the conformation of CALES, while the CALAM conformation in the film was altered when Cd^{2+}, Cu^{2+} Na^{+}, or K^{+} were present in the subphases.

The alignment of the CH_2 groups in the chains of CALES and CALAM parallel to the surface of the film was clearly indicated by an increase in the relative intensity of both the symmetric and antisymmetric stretching vibrations in the transmission IR spectra of the LB films.

CALES shows no significant change in the limiting area with changes in the subphase, but it has been clearly shown by spectroscopic techniques that metal cations are incorporated into the LB film.

Acknowledgment. Funding for this project was provided by the Natural Sciences and Engineering Research Council of Canada (P.J.D. and R.A.), Fundação de Amparo à Pesquisa do Estado de São Paulo–Brazil (W.M.), the Universidade Federal de São Carlos, and the University of Windsor.

LA950055S